

Phase Transitions and Kinetics of Vapour Adsorption on Mesoporous Silica

Zhuan-Tao He, Chun-Mei Wu*, Wei Zhang, You-Rong Li

Key Laboratory of Low-grade Energy Utilization Technologies and Systems of Ministry of Education, School of Energy and Power Engineering, Chongqing University, Chongqing 400044, China

(Corresponding Author: Chun-Mei Wu, Email: chunmeiwu@cqu.edu.cn)

ABSTRACT

To investigate the phase transitions during adsorption and kinetics of vapor adsorption on mesoporous silica, a series of molecular simulations are conducted in this work. The results provide new insights into the formation of liquid bridges and the growth of cavitation bubbles. The liquid is in a metastable state during desorption, with evaporation potentially occurring through meniscus retreat or cavitation. Spontaneous formation of tiny bubbles is observed in the liquid phase. Multiple tiny bubbles often form in proximity, indicating their interdependence. Eventually, as evaporation continues to increase, these bubbles coalesce into ones, initiating the nucleation mechanism for the liquid-to-vapor transition of a metastable liquid.

Keywords: phase transitions; liquid bridge, cavitation, thermodynamics

1. INTRODUCTION

Confinement is known to induce many extraordinary physical properties that are not observed in bulk systems. Therefore, gaining a deep understanding of fluid behavior at the nanoscale is crucial for various applications, including biotechnology [1], drug delivery [2], carbon dioxide storage [3], and oil production [4]. Microporous and mesoporous materials, crucial in industrial processes, especially as catalysts, demand comprehensive characterization encompassing specific surface area, pore size distribution, and porosity for effective utilization. Furthermore, there is an urgent need for a thorough understanding of adsorption and phase transitions on mesoporous.

Numerical simulation and experimental methods are commonly employed to investigate changes in fluid phase behavior. Numerical simulation encompasses equations of state [5], molecular dynamics simulation [6] and density functional theory [7], while experimental methods involve differential scanning calorimetry [8] and gas physical adsorption [9]. Recent advancements in

lab-on-a-chip (LOC) technology have facilitated the observation of phenomena such as vapor bubble nucleation [10], interface growth and gas-liquid phase transformation [11] in porous media, leading to the emergence of a new research paradigm. However, the kinetic process of vapor adsorption significantly influences the fluid phase transition of mesoporous materials. Given the challenge of providing a detailed and accurate description of adsorption behavior, accurately predicting the transition from adsorption to capillary condensation under experimental conditions remains difficult.

In conclusion, while researchers have extensively studied related aspects, the kinetics of vapor and the transition mechanisms from adsorption to capillary condensation remain incompletely understood. To address this, we systematically examine vapor adsorption and phase transitions on mesoporous silica from a microscopic perspective. Through theoretical analysis and molecular dynamics simulations, we unveil the crucial role of pore filling in the capillary condensation process during adsorption of mesoscopic materials. Additionally, the thermodynamic stability of the adsorbate is discussed.

2. PHYSICAL MODEL AND SIMULATION METHOD

The configuration of nitrogen adsorption on mesoporous silica, with dimensions of 31.2×6.2×6.2 nm in the x , y , and z direction, is depicted in Fig. 1. Amorphous silica is prepared from fully dense crystalline silica using a melt-quench method [12]. This procedure involves initialization, heating to super-high temperature, followed by quenching to ensure sufficient amorphicity. The resulting radial distribution function and relevant bond parameters in the amorphous structure align well with existing literature data [13]. The nanopore is subsequently created by removing atoms in a cylindrical region of diameter $d = 3.3$ nm. The Si/O ratio is then confirmed to achieve a ratio of 1:2, with a

This is a paper for the 16th International Conference on Applied Energy (ICAE2024), Sep. 1-5, 2024, Niigata, Japan.

corresponding slicing diagram of amorphous mesoporous silica showed in Fig. 1(b).

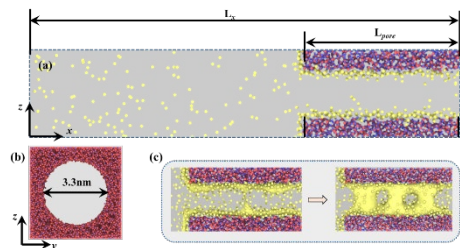


Fig. 1. Physical model of mesoporous silica

To describe the interaction of amorphous silica, we employ a modified Tersoff potential. Nitrogen molecule is modeled as a single Lennard-Jones sphere with the $\epsilon_{\text{Nf}}=0.0082$ eV and $\sigma_{\text{Nf}}=3.75$ Å. Interactions with silicon and hydrogen atoms of the substrate are disregarded due to low polarizability [14], and only Lennard-Jones interactions between the nitrogen molecule and the oxygen atoms of the silica substrate are considered. The cross-parameters for the interaction between the nitrogen molecules and the oxygen atoms of the pores were determined using the Lorentz-Berthelot mixing rules. Periodic boundary conditions are imposed in the x and y directions, and fixed boundary conditions are applied in the z direction. A time step of 2 fs was used for all simulations, with a cutoff set at $3.5\sigma_{\text{Nf}}$.

3. RESULTS AND DISCUSSIONS

3.1 Pore filling and capillary condensation transition

To present the kinetics of phase transition, the snapshots of nitrogen in the silica cylindrical nanopore throughout adsorption process are demonstrated in Fig. 2.

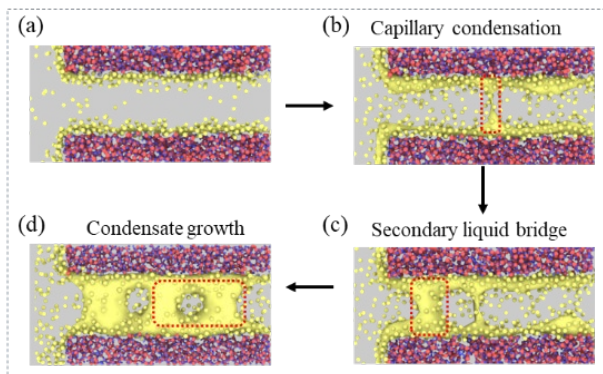


Fig. 2. Snapshots of adsorption and capillary condensation of nitrogen in the mesoporous silica

During adsorption, as relative pressure increases, the thickness of the adsorbed liquid film progressively increases along the solid wall. When the thickness of the two parallel films reaches a critical value, the liquid molecules begin to attract the molecules on the opposite walls. This attraction prompts the adsorbed film to spontaneously form a liquid bridge, as shown in Fig. 2(b). A secondary liquid bridge forms as a result of adsorption at a pressure further increases (Fig. 2(c)). Consequently, the formation of this bridge accelerates the overall pore filling rate, suggesting its role as a nucleation center, thereby triggering further condensation at the pore edge. Subsequently, condensation progresses rapidly (Fig. 2(d)), ultimately filling the nanopore with liquid.

3.2 Density distribution of nitrogen in mesoporous silica

Figure 3 illustrates the density distribution of nitrogen in the mesoporous silica under varying pressure ratios, with the region $z > -70$ Å representing the pore position. The peak density, occurring at $z = -70$ Å for $x^V = 0.14$, reaches approximately 6.9 mol·L⁻¹. With the ongoing increase in pressure ratio, a second peak density emerges around $z = -33$ Å, while the initial peak density declines to 5.2 mol·L⁻¹. This suggests a preferential accumulation of nitrogen on the outer surface of the nanopore entrance, forming an adsorption layer due to gas-solid interaction. As the pressure ratio rises and the adsorption progresses, nitrogen continues to adsorb into the pore, causing the adsorption layer to expand.

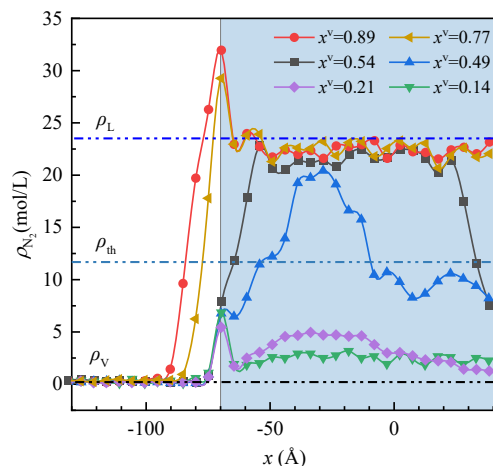


Fig. 3 Density distribution of nitrogen in mesoporous silica

The adsorption layer on the outer surface acts as a contributor to the adsorption occurring in the pore, leading to a reduction in thickness and a decline in the initial density peak observed. At the pressure ratio of

0.49, the density near $z = -33 \text{ \AA}$ falls in the range defined by ρ_{th} ($\rho_{th}=1/2(\rho_v + \rho_L)$) and the density ρ_L of the saturated liquid phase. This observation suggests the onset of capillary condensation in the pores and the formation of liquid bridging. As the pressure ratio is further increased, the filling rate inside the pore accelerates due to the rapid growth of the liquid bridge, bringing the density inside the pore closer to that of the saturated liquid.

3.3 Thermodynamic stability of the adsorbate

Following the capillary condensation, the liquid phase occurs in the pore. As fluid condensate accumulates, it gradually expands towards the pore, forming a meniscus. Local equilibrium at the liquid-vapor interface demands equal chemical potentials between vapor and liquid phases, in accordance with the Young-Laplace equation [15]. Simplifying, we obtained

$$r_p = \frac{2\gamma^{LV} \cos \theta}{\left(P_v - P_s - \frac{RT \ln x^v}{v} \right)} \quad (1)$$

where v denotes the specific volume of the pure liquid at saturation.

Eq. (1) allows for the calculation of the relationship between the contact angle and pressure ratio, as depicted in Fig. 4.

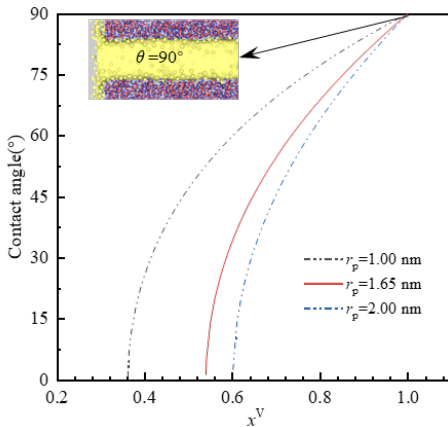


Fig. 4 The contact angle of the condensate at the pore mouth varies with the pressure ratio

It's observed that when the gas phase pressure reaches saturation pressure, the pore becomes completely filled with adsorbent, resulting in a contact angle of 90° at the liquid-vapor interface. During desorption, as the vapor phase pressure decreases, condensate liquid in the pore begins to diffuse into the gas phase, forming a meniscus in the pore mouth. As desorption progresses and the contact angle at the

liquid-vapor interface approaches 0° , the liquid-vapor interface transitions to a hemispherical shape.

Vapor pressure ratio, x^v , and liquid pressure ratio, x^l , can be converted to each other [15]

$$x^l = \frac{RT \ln(x^v)}{vP_s} + 1 \quad (2)$$

Therefore, x^l can be calculated as a function of θ , as shown in Fig.5. We observe that the liquid phase pressure becomes negative when the contact angle is 0 , indicating the metastability of the liquid phase. Classical capillary condensation suggests that the vapor-liquid transition is delayed due to the presence of metastable adsorption films associated with the nucleation barrier that forms the liquid bridge. In a pore filled with a liquid-like condensate, where a liquid-vapor interface already exists, evaporation/desorption occurs through a receding meniscus. Essentially, the desorption process is connected to the equilibrium vapor-liquid transition. The details of the adsorbate behavior during desorption depend on the thermodynamic state of the pore fluid and the structure of the adsorbate.

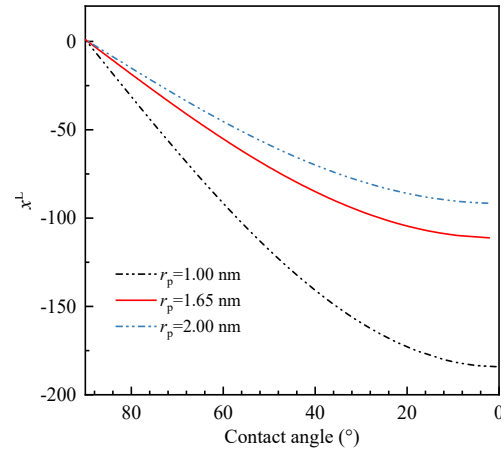


Fig. 5 The pressure in the liquid phase of condensed nitrogen in pores plotted against the contact angle.

To understand the desorption process from a microscopic perspective, Fig. 6 illustrates the underlying dynamics of nitrogen desorption in a mesoporous silica pore.

Desorption occurs from the mouth of the nanopore into the cavity. Initially, the liquid in the mouth evaporates, gradually moving towards the center of the nanopore where the vapor-liquid interface, known as the meniscus, forms. This continuous evaporation process is evidenced by the retreat of the meniscus from the nanopore entrance, as illustrated in Fig. 6(a). Concurrently, as pressure decreases, nucleation of vapor bubbles is observed, referred to as mixed "discontinuous

evaporation". The decrease in pressure leads to the spontaneous formation of tiny bubbles in the liquid (Fig. 6(b)), which expand and coalesce as evaporation continues, resulting in the formation of cavities in mesoporous silica (Fig. 6(c-d)). This phenomenon, in which bubble growth occurs through the formation of multiple cavitation bubbles that combine to form larger bubbles, signifies the transition from liquid to vapor via nucleation. These observations corroborate the findings of Neimark et al. [16]. Similarly, Jatukaran et al. [17] have documented this occurrence in experiments involving propane evaporation in two-dimensional (2D) nanoporous media less than 10 nm in size.

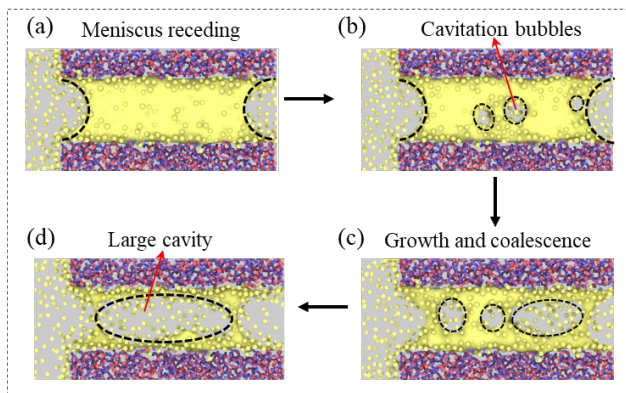


Fig. 6 Typical molecular configuration of N_2 desorption in mesoporous silica

4. CONCLUSIONS

In this paper, we combine molecular dynamics simulations and theoretical analysis to capture the dynamic evolution of gas adsorption and pore filling in mesoporous silica from a microscopic point of view. The transition between the adsorbed state and the capillary condensate of the gas in the mesoporous pore has been elucidated, and the stability of the liquid phase in the mesoporous pore has been analyzed. The main conclusions are as follows:

(1) As the relative pressure increases during adsorption, the thickness of the adsorbed liquid film along the solid wall progressively expands. Upon reaching a critical thickness for the two parallel films, intermolecular attraction prompts the spontaneous formation of a liquid bridge, as liquid molecules on opposing walls begin to attract each other. Subsequent pressure increments lead to the formation of secondary liquid bridges, accelerating the overall pore filling rate and serving as nucleation centers that induce additional condensation at the pore edge. This process ultimately

results in rapid condensation, effectively filling the nanopore with liquid.

(2) The liquid in the pore remains in a metastable state during desorption. Desorption initiates from the mouth of the nanopore, extending into the cavity. Two evaporation modes are evident: continuous evaporation, where the meniscus gradually recedes, and discontinuous evaporation, triggered by vapor bubble nucleation. In the latter case, evaporation and cavitation bubble formation occur almost instantly with pressure reduction. These bubbles subsequently expand and merge to form a larger cavity.

ACKNOWLEDGEMENT

This work is supported by the National Natural Science Foundation of China (51876012) and Natural Science Foundation of Chongqing (CSTB2024NSCQ-MSX1065).

REFERENCE

- [1] Noreen S, Maqbool A, Maqbool I, et al. Multifunctional mesoporous silica-based nanocomposites: Synthesis and biomedical applications. *Materials Chemistry and Physics*. 285 (2022): 126132.
- [2] Alberti S, Schmidt S, Hageneder S, et al. Large-pore mesoporous silica: template design, thin film preparation and biomolecule infiltration. *Materials Chemistry Frontiers*. 2023, 7(18): 4142-4151.
- [3] Sani S, Liu X, Stevens L, et al. Amine functionalized lignin-based mesoporous cellular carbons for CO₂ capture. *FUEL*. 2023, 351:128886.
- [4] Yuan L, Zhang Y, Liu S, et al. Molecular dynamics simulation of CO₂-oil miscible fluid distribution and flow within nanopores. *Journal of Molecular Liquids*. 2023,380:121769.
- [5] Alloush R M, Sharma K V, Piri M. The effect of confinement on the phase behavior of propane in nanoporous media: an experimental study probing capillary condensation, evaporation, and hysteresis at varying pore sizes and temperatures. *Physical Chemistry Chemical Physics*. 2024, 26(7): 5978-5985.
- [6] Fu R, Li J, Huang Z. Intervening liquid-vapor interface with atomically thin nanopore-film to manipulate kinetically limited evaporation. *Journal of Molecular Liquids*. 2023, 385: 122410.
- [7] Sidorenkov A, Aslyamov T, Ilinov D, et al. Methane storage in nano-pores: Molecular dynamics simulation and density functional theory. *Geoenergy Science and Engineering*. 2023, 222: 211419.
- [8] Yang H, Jayaatmaja K, Qiu X, et al. Accurate Measurement of the Isothermal Heat of Capillary

Condensation in Nanopores Using Differential Scanning Calorimetry and Adsorption / Desorption Experiments. *Journal of Physical Chemistry C*. 2023,127(45):21980-8.2023.

[9] Emelianova A, Balzer C, Reichenauer G, et al. Adsorption-Induced Deformation of Zeolites 4A and 13X: Experimental and Molecular Simulation Study. *Langmuir*. 2023, 39(32): 11388-11397.

[10] Bao B, Zandavi S H, Li H, et al. Bubble nucleation and growth in nanochannels. *Physical Chemistry Chemical Physics*. 2017, 19(12): 8223-8229.

[11] Yang Q, Jin B, Banerjee D, et al. Direct visualization and molecular simulation of dewpoint pressure of a confined fluid in sub-10 nm slit pores. *Fuel*. 2019, 235: 1216-1223.

[12] Meng F, Elshahhat M, Liu J, et al. Thermal resistance between amorphous silica nanoparticles. *Journal of Applied Physics*. 2017, 121:194302.

[13] Zhang S, Perez-Page M, Guan K, et al. Response to Extreme Temperatures of Mesoporous Silica MCM-41: Porous Structure Transformation Simulation and Modification of Gas Adsorption Properties. *Langmuir*. 2016, 32(44): 11422-11431.

[14] Coasne B, Galarneau A, Di Renzo F, Pellenq RJ. Molecular simulation of nitrogen adsorption in nanoporous silica. *Langmuir*. 2010, 26(13):10872-81.

[15] Zandavi S H, Ward C A. Contact angles and surface properties of nanoporous materials. *Journal of Colloid and Interface Science*, 2013, 407: 255-264.

[16] Neimark A V, Vishnyakov A. The birth of a bubble: A molecular simulation study. *Journal of Chemical Physics*. 2005, 122(5).

[17] Jatukaran A, Zhong J, Persad A H, et al. Direct Visualization of Evaporation in a Two-Dimensional Nanoporous Model for Unconventional Natural Gas. *ACS Applied Nano Materials*. 2018, 1(3): 1332-1338.